A soft chemistry route to prepare hybrid ZnO nanostructured films with a lamellar structure

Benoît P. Pichon,[ab] Aude Mezy,[a] Jean-Claude Tedenac,[a] Didier Tichit[a] and Corine Gérardin*[a]

Received (in Montpellier, France) 24th July 2009, Accepted 14th September 2009
First published as an Advance Article on the web 2nd October 2009
DOI: 10.1039/b9nj00365g

A soft chemistry route involving SDS and zinc salt aqueous solutions allowed growing films of hybrid ZnO-based nanostructured plates from a substrate with ZnO crystal seeds. Plates exhibit a long-range ordered lamellar nanostructure formed of thin ZnO layers and SDS bilayers and remarkably, the lamellar phase presents a unique interlayer distance. Moreover, evidence of the ZnO phase in the confined interlamellar space is provided. The hybrid lamellar structure may result from a cooperative organization of surfactants and zinc molecular species into two-dimensional structures involving SDS assembling and charge screening of the surfactant head groups by zinc polycationic species. DS^- surfactants not only prevent ZnO crystal growth in the direction of the *c*-axis, as hydrosoluble complexing agents do, but they also promote the formation of a mesostructured hybrid lamellar phase. The very simple wet chemical route described here may constitute a valuable alternative to the electrodeposition and pulsed laser ablation processes.

1. Introduction

Nanostructured zinc oxide-based films with controlled sizes and morphologies are of great interest for numerous applications in optics and electronics, or as sensors and dye-sensitized solar cells.[1] For example, properties of ZnO systems used as lasers[2] can be improved by quantum confinement effects,[3] which directly depend on the structure at the nanometre scale of the grown objects.[4] ZnO is also well known for its applications in both photoconduction and photovoltaics. Recently, M. Sofos *et al.* have shown the great interest in highly ordered nanostructured hybrid ZnO based materials as photoconductors; they prepared, by electrodeposition, nanoscale lamellar photoconductor hybrids combining complementary *p*-type organic and *n*-type inorganic components.[5] Different methods have been previously developed to prepare ZnO films like chemical vapour deposition,[6] pulsed laser ablation[7] or sputtering.[8] Few of them use soft chemical reactions in aqueous solution despite the well known advantages like a better control of nucleation and growth processes occurring at a moderate temperature. Template based syntheses have been previously used in the preparation of metal oxide based hybrid films. Organized micellar assemblies enable controlling the growth kinetics of inorganic phases due to specific interactions between organic moieties and inorganic precursors.[9] Applications of the hybrid films are determined by the properties of both, the organic and inorganic substructures.

ZnO is a wide band gap (3.37 eV) semiconductor, which possesses unique electrical and optical properties. It has a wurtzite crystal structure, which results in an elongated hexagonal crystal habit along the *c*-axis.[10] Large arrays of well-aligned ZnO based low-dimensional structures like nanorods have been grown from various substrates by a wet chemical method.[11,12] In addition, organic species were found to control crystal growth when adsorbing on crystal faces with the highest free energy. For instance, surfactants were found to modify the morphology of nanorods (width, aspect ratio),[3,13–15] while citric acid[16] or polymers[17] lead to a plate-like morphology. Recently, the use of sodium dodecyl sulfate (SDS) combined with the electrodeposition method[18] led to the production of hybrid ZnO continuous films with lamellar structures. The films exhibit a poorly ordered structure and an ill-defined morphology of the nanoparticles. In comparison, the laser pulsed ablation technique lead to the formation of better-defined platelets with a similar layered structure.[19] However, these preparation routes require specific equipment, the control of several parameters and the presence of the ZnO phase is not always evidenced. These observations were an incitement to develop a simple soft chemistry route for the preparation of thin films of lamellar hybrid ZnO plates. The approach we propose here only requires controlling the nature of the structuring agent and the concentration of the reactants, which is a significant advance in the synthesis of hybrid lamellar ZnO structures.

2. Experimental

Starting materials were analytical-grade, zinc nitrate hexahydrate $Zn(NO_3)_2{\cdot}6H_2O$ (Aldrich), hexamethylenetetramine (HMTA) (Merck, Germany), sodium dodecyl sulfate (SDS) (Merck,

[a] *Institut Charles Gerhardt Montpellier-UMR 5253 CNRS-ENSCM-UM2-UM1, 8 rue de l'Ecole Normale, 34296 Montpellier Cedex 5, France. E-mail: corine.gerardin@enscm.fr; Fax: +33 (0)4 67 16 34 70; Tel: +33 (0)4 67 16 34 65*
[b] *Institut de Physique et de Chimie des Matériaux de Strasbourg-UMR 7504 (CNRS/ULP/ECPM), 23 rue du Loess-BP 43, 67034 Strasbourg Cedex, France*

Germany) and cetyl trimethylammonium bromide (CTAB) (Acros Organics). All materials were used as received without further purification. Deionized water with a specific resistivity exceeding 5 MΩ was used.

ZnO nano-objects were grown onto films of oriented zinc oxide nanoparticles, which act as crystal seeds. First, ZnO nanoparticles were formed onto a glass substrate following a sol-gel process. Glass substrates were dip-coated 5 times into a colloidal solution containing $Zn(OAc)_2$, diethanolamine and water with a (1:1:5) molar ratio in propanol ([Zn] = 0.2 M). Afterwards, thermal decomposition of the film at 500 °C for 2 h lead to the obtention of a 400 nm to 1 mm thick film of ZnO crystal seeds.

The growth of nano-objects was then performed onto the ZnO substrate in 25 mL of a 2.5×10^{-2} M equimolar aqueous solution of $Zn(NO_3)_2{\cdot}6H_2O$, HMTA and surfactant (CTAB or SDS) when required. The substrate was placed upside down in a vial containing the mixture in order to prevent any deposition of objects grown from the solution. The system was placed in an oven for 15 h at 90 °C in order to induce the crystallization of ZnO. The substrate was then rinsed with water and dried in air at 80 °C for 8 h. The colloidal suspension and precipitate formed in solution were centrifuged and then washed by redispersion in deionized water before drying at 80 °C.

Zinc oxide structures grown from substrates and powders collected from solution were observed by scanning electron microscopy (SEM), they were mounted onto aluminium stubs with double-sided carbon tape. The specimens were observed with a Hitachi type S-4500 I scanning electron microscope, using a cold cathodic emission field at an accelerating voltage of 2 kV. Energy dispersive X-ray (EDX) diffraction analysis of the arrays coupled to the field-emission scanning electron microscope was performed at 15 kV with a resolution of 1 mm coupled to a scanning electron microscope LEO type S260. Transmission electron microscopy (TEM) was performed using a JEOL 1200 EXII electron microscope operating at an accelerating voltage of 80 kV. Structures grown on solid substrates were scraped and dispersed in ethanol in an ultrasonic bath. A drop of the suspension was deposited on a carbon coated TEM grid. The excess of solvent was removed by contact on the side of the grid with filter paper. After drying for 5 min at room temperature, the samples were inserted in the microscope. Selected area electronic diffraction (SAED) was performed on a JEOL 1200 EXII electron microscope operating at an accelerating voltage of 80 kV with a camera length of 80 cm. The samples were the same as the ones prepared for TEM and were studied at the same time TEM micrographs were recorded. The crystalline phase of the materials was determined by X-ray Diffraction (XRD) using a Bruker D8 Advance with a Cu $K_{\alpha 1}$ (1.540598 Å) radiation in the [0.6–60°] 2θ range, with a step of 0.02° and a step time of 1 s. Fourier transform infrared spectroscopy (FT-IR) reflection measurements were recorded directly on glass substrates covered with zinc structures from 600 to 4000 cm^{-1} with a Bruker Equinox spectrometer using a DRIFT Spectratech cell and equipped with a MCT detector. Powders collected from solution were analyzed in the form of KBr pellets. FT-IR transmission measurements were recorded using a Bruker Vector 22 FTIR spectrometer from 400 to 4000 cm^{-1}. Both types of spectra were recorded by acquiring 16 scans with a resolution of 4 cm^{-1}.

3. Results

The present synthesis method consists in precipitating zinc ions with HMTA in the presence of SDS and of a continuous film of ZnO crystal seeds preformed on a substrate. The mean size of the nanoparticle seeds of the substrate was determined by scanning electron microscopy (SEM), it equals 33 ± 3 nm (Fig. 1a and d).

SEM images show that the film is formed of densely packed nanostructures with a plate-like morphology (Fig. 1b). The plates are quite uniform in size, with a length of up to 20 μm and a width of up to 5 μm. A cross-sectional SEM view of the plates (Fig. 1c) shows that the thickness of the plates amounts to 95 ± 5 nm and that those close to the surface clearly grow from the ZnO seeds (Fig. 1e). The transmission electron microscopy (TEM) image reveals a well-ordered layered nanostructure with a lamellar spacing of about 3.1 nm (Fig. 1f).

The nanostructure of the film was also investigated by XRD. The diffractogram (Fig. 2a) is typical of a highly ordered lamellar structure, as revealed by the presence of nine harmonics for the (001) Bragg reflections. Their positions correspond to an interlayer distance of 3.04 nm, in agreement with TEM. Such results suggest a hybrid lamellar structure formed by ZnO layers intercalated with dodecylsulfate (DS^-) surfactant ions.

The objective was then to confirm the exact nature of the constituents of the lamellar assembly. The presence of the ZnO seeds impedes a clear assignment of the X-ray diffractogram of the hybrid mesostructured plates grown onto the substrate, due to X-ray reflections coming from the ZnO substrate. This was an incitement to form the hybrid structure also directly by precipitation from an homogeneous solution, *i.e.* in the absence of a ZnO substrate. We checked by XRD (Fig. 2b), SEM (Fig. 3a) and TEM (Fig. 3b) that the plates obtained from solution exhibit the same lamellar structure as the ones grown from the ZnO seeds. In the XRD patterns (Fig. 2) of both samples grown in different conditions, five diffraction peaks were observed in the wide angle region (30° to 60° 2θ range). They are assigned to the hexagonal wurtzite structure ZnO (JCPDS, card no 36–1451, $P63mc$, a = 3.2495 Å, c = 5.2069 Å). In particular, the three more intense diffraction

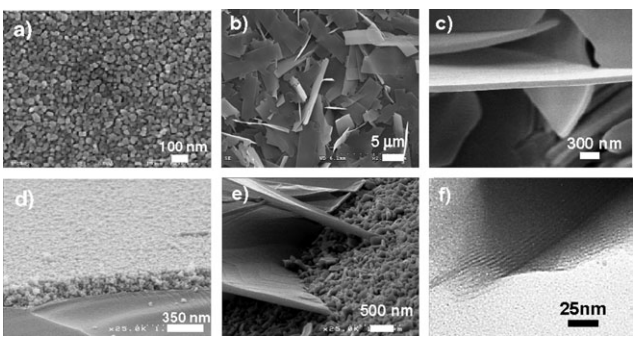

Fig. 1 (b,c,e) SEM and (f) TEM images of ZnO based-hybrid plates grown in the presence of SDS from (a,d) the substrate of ZnO nanoparticles.

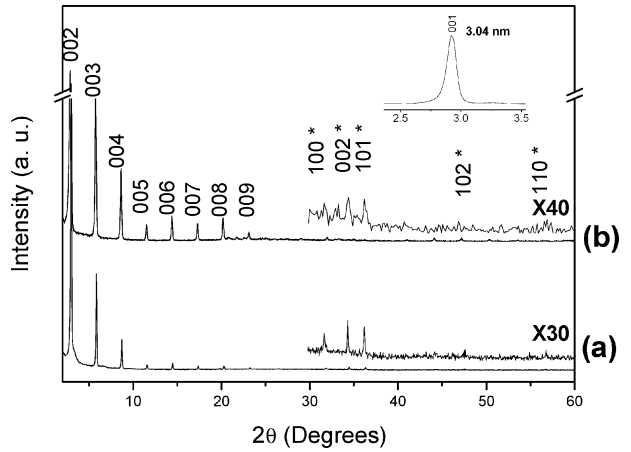

Fig. 2 XRD patterns of ZnO hybrid plates grown (a) in the presence of SDS onto the ZnO crystal seeds and (b) in the bulk of the solution. Inset: (001) reflection of the lamellar structure of (a).

peaks can be assigned to reflections on (100), (002) and (101) crystal planes. In contrast to what Liang *et al.* reported on layered zinc hydroxide/SDS structure grown by pulsed-laser ablation,[20] there is no peak assigned to the β-$Zn(OH)_2$ phase in the present results. Therefore, the problem of the contribution of the ZnO seeds in the XRD pattern of the plates grown onto the substrate being overcome, it was shown that the inorganic part of the hybrid lamellar structure is made of ZnO layers.

An EDX analysis of the plates grown in solution shows sulfur and zinc in addition to carbon and oxygen elements (Fig. 3c). It indicates the presence of both dodecylsulfate surfactants and ZnO components with a molar ratio of 1:3. The FT-IR spectrum (Fig. 4) shows vibrational bands that are also due to the presence of both components. At 490 cm^{-1}, the νZn–O mode is observed. Moreover, the broad IR band between 3400 and 3580 cm^{-1} indicates the presence of hydroxyl

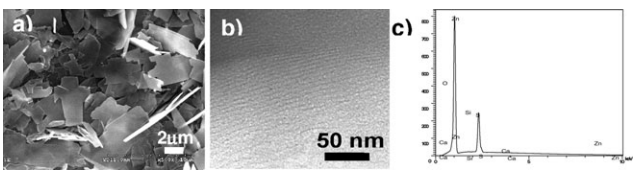

Fig. 3 Hybrid plates grown in the solution in the presence of SDS. (a) SEM and (b) TEM pictures, and (c) EDX-analysis

groups that are probably present at the surface of the ZnO layers. The band around 1619 cm^{-1} is due to δH_2O vibration of absorbed water molecules. A narrower band (3344 cm^{-1}) is observed and may correspond to the interaction of the sulfate groups with the Zn species. The presence of DS^- ions is highlighted by specific vibration modes corresponding to alkyl chains (CH_2 at 2854, 2870, 2922 and 2955 cm^{-1}) and sulfate groups (OSO_3^- at 1061 and 1191–1234 cm^{-1}). The bathochromic shift of OSO_3^- stretching bands relative to free SDS micelles in solution is in good agreement with the DS^- anionic surfactant absorbed onto ZnO polycationic layers by electrostatic interactions. Similar interactions have been previously reported between SDS and Al_2O_3 surface by Sperline *et al.*[21] After washing the structure with ethanol, DS^- vibration modes are still present in the spectrum (data not shown), which is indicative of strong interactions.

All the previous features allow concluding that the plates are formed of alternating ZnO and DS^- layers. The interlamellar distance of the hybrid structure is found to be very close to the thickness of DS^- bilayers, *i.e.* about 3 nm (twice the length of a fully stretched DS molecule, 1.5 nm), revealing that the ZnO phase is very thin. The observation of nine harmonics in the XRD pattern shows the long range order of the lamellar structure, which is related to the large size of the intercalated entity. Its coherence length, calculated by the Scherrer formula, was found to be 94 nm; it corresponds to about 30 times the interlayer distance (3.0 nm) and is in good agreement with the plate thickness determined by SEM (95 ± 5 nm). Remarkably, the individualized platelets obtained here exhibit a well-defined morphology and a high degree of crystallinity.

In order to investigate the effect of SDS, the experiment was performed in a surfactant-free medium and with the cationic cetyl trimethyl ammonium bromide (CTAB). The absence of SDS has a dramatic effect on the characteristics of the film. As it was previously reported in the absence of surfactant,[11a] SEM images show that the whole film of ZnO nanoparticles was covered with densely packed nanorods (Fig. 5a and c). They display a hexagonal section and an orientation perpendicular to the substrate. The presence of CTAB (Fig. 5b and d) leads only to a change of the rod mean diameter, which increases to 160 ± 80 nm compared to 80 ± 5 nm in a surfactant free medium.

In addition, XRD patterns (Fig. 6) exhibit diffraction peaks, which can be indexed as ZnO. The higher intensity of the (002) reflection compared to that of (100) and (101) reflections

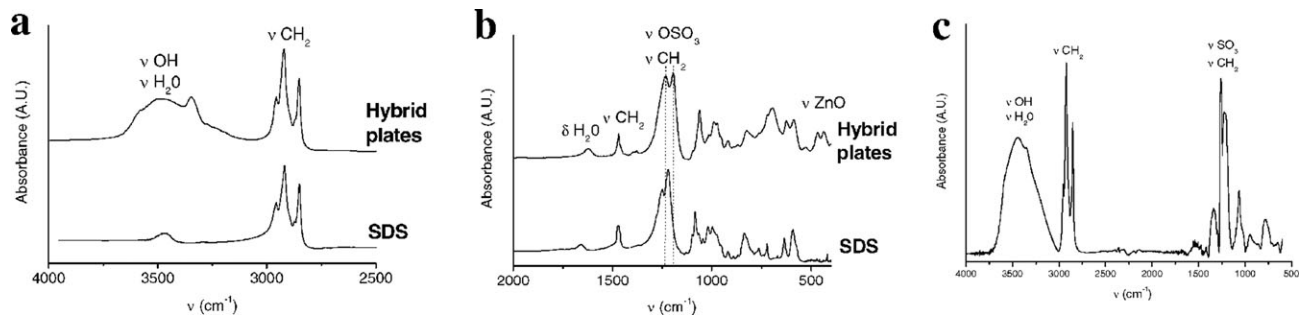

Fig. 4 FT-IR spectra of (a,b) hybrid plates grown in solution in the presence of SDS and of pure SDS surfactant and (c) hybrid plates grown onto the film of ZnO nanoparticles.

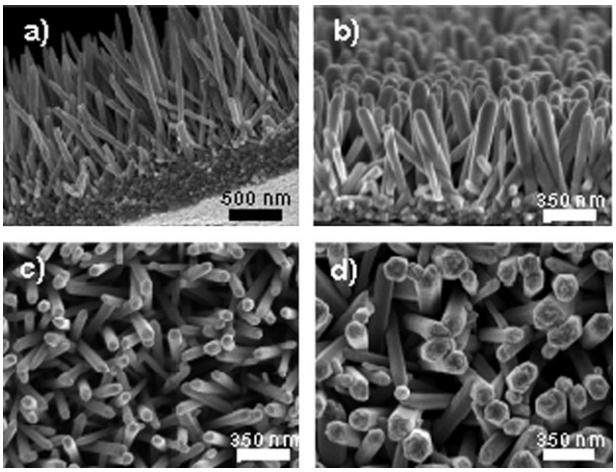

Fig. 5 SEM images. (a,b) Side-views and (c,d) top-views. ZnO nanorods grown onto the ZnO nanoparticles (a,c) without surfactant and (b,d) in the presence of CTAB.

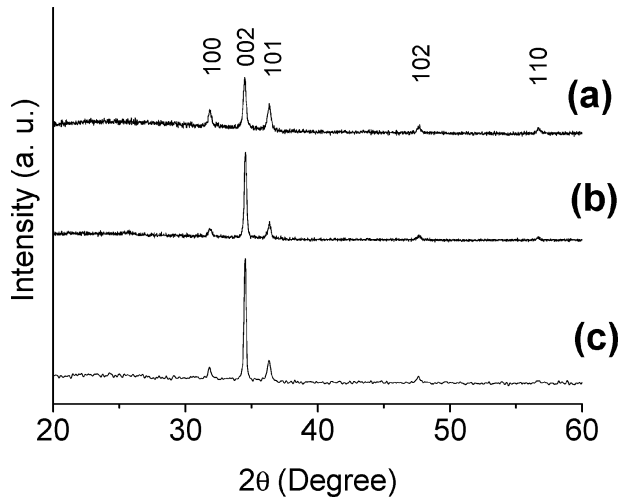

Fig. 6 X-Ray diffraction patterns collected from (a) the film of ZnO nanoparticles deposited on the glass substrate before reaction and after reaction (b) without surfactant and (c) in the presence of CTAB.

reveals a preferential orientation along the *c*-axis. The relative increase in intensity of the (002) reflection in (Fig. 6b) and (Fig. 6c) is consistent with the growth of ZnO rods along the *c*-axis. TEM experiments (Fig. 7a) combined with SAED analysis (Fig. 7b) show that the rods formed in a surfactant free medium are ZnO single crystals, which are grown along the *c*-axis from the substrate.

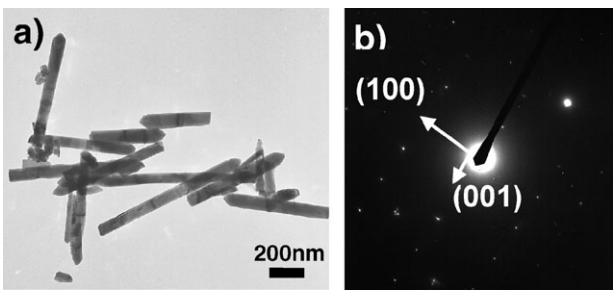

Fig. 7 Nanorods grown onto the film of ZnO nanoparticles. (a) TEM picture and (b) SAED pattern.

The kinetics of the reaction are controlled by the increase of the temperature in the synthesis solution, which results in the hydrolysis of HMTA and the production of ammonia.[22] It induces hydrolysis of zinc cations and the formation of polycationic zinc hydroxide species ($Zn(OH)_n^{(2-n)+}$) in solution directly followed by the formation of a zinc oxide structure. The presence of hydrosoluble zinc complexing additives prevents crystal growth in the direction of the *c*-axis. Their adsorption onto the ZnO (001) plane leads to one-dimensional ZnO structures or to platelet morphologies.[23] The present results reveal that SDS molecules behave differently from hydrosoluble complexing agents due to their amphiphilic character. They self-assemble into micelles of varying shapes when at a higher concentration than the critical micellar concentration (CMC). The presence of zinc polycationic species increases the ionic strength and tends to reduce the CMC. Depending on the composition of the solution and on the ionic strength, spherical SDS micelles may transform into elongated micelles or lamellae.[24] The synthesis presented here was performed at a SDS concentration (2.5×10^{-2} M) above the CMC (7×10^{-3} M).[25] This value is given at room temperature and our experiment occurs at 90 °C, but it is known that CMC values present very small variations with temperature.[26] ZnO crystal seeds, which are preferentially oriented along the *c*-axis, present a positively charged surface. Thus, that surface may interact with the negatively-charged headgroups of the DS^- molecules. Interaction of DS^- micelles with positively charged faces of ZnO seeds lead then to the organization of the DS^- surfactant micelles into bilayers.[27]

It suggests that the direct oriented growth from the ZnO crystal seeds is inhibited by a bilayer of DS^- surfactants, which covers their whole surface. In addition, the sulfonate headgroups constitute an activated surface on which polycationic zinc species adsorb and initiate the growth of a subsequent inorganic layer. Taking into account the relatively thin layer of ZnO, we can suggest that the formation of the ZnO phase occurs by condensation of the polycationic zinc species confined in the two-dimensional interlayer space of DS^-. Consecutive DS^- bilayers may act as the walls of a nanoreactor, where entrapped zinc polycationic species condense into ZnO when pH conditions are fulfilled by HMTA decomposition. In addition, the preferential orientation of the seeds along the *c*-axis could contribute to direct the orientation of the plates in a direction parallel to the substrate.

Therefore the hybrid lamellar structure may result from a cooperative organization of organic and inorganic molecular species into two-dimensional structures involving surfactant assembling and charge screening of the surfactant head groups by zinc entities. DS^- surfactants not only prevent crystal growth in the direction of the *c*-axis, as hydrosoluble complexing agents do, but they also act as structuring agents and induce a cooperative process of precipitation of a hybrid lamellar structure at the surface of the substrate.

In conclusion, it has been shown that the formation of well crystallized ZnO hybrid lamellar structured films can be obtained by using an anionic surfactant in a seeded growth process. The ability of SDS to form DS^- bilayers and to

complex polycationic zinc species allows to simultaneously inhibit the growth of ZnO along the *c*-axis and to promote the formation of hybrid mesophases. Films of long range-ordered DS^-/ZnO nanostructures are thus obtained, and remarkably, the lamellar hybrid nanostructures exhibit a unique interlayer distance. Moreover, evidence of the ZnO phase in the confined interlamellar space is provided. The very low thickness (about 1 nm) of the ZnO layers may lead to interesting quantum confinement effects. An interesting extension of the present work could also be to use functional organic templates, such as electronically active conjugated surfactant moieties in order to enhance optical properties of the hybrid systems. The formation mechanisms and the properties of such films have to be further investigated and will be reported in a forthcoming paper. At last, the very simple wet chemical route described here constitutes a valuable alternative to the electrodeposition and pulsed laser ablation processes. It allows performing controllable and well-repeatable syntheses in mild aqueous conditions, which are consistent with requirements for industrial developments.

Acknowledgements

This work was supported by the Ministère de la Recherche under the ACI NANOZINOX.

References

1 (*a*) Z. Tang, G. Wong, P. Yu, M. Kawasaki, A. Ohtomo, H. Koinuma and Y. Segawa, *Appl. Phys. Lett*., 1998, **72**, 3270; (*b*) L. Guo, Y. L. Ji, H. B. Xu, P. Simon and Z. Y. Wu, *J. Am. Chem. Soc*., 2002, **124**, 14864; (*c*) A. B. Djurišić and Y. H. Leung, *Small*, 2006, **2**, 944.
2 M. H. Huang, S. Mao, H. Feick, H. Yan, Y. Wu, H. Kind, E. Weber, R. Russo and P. Yang, *Science*, 2001, **292**, 1897.
3 L. Yanhong, W. Dejun, Z. Qidong, Y. Min and Z. Qingli, *J. Phys. Chem. B*, 2004, **108**, 3202.
4 J. T. Hu, T. W. Odom and C. M. Lieber, *Acc. Chem. Res*., 1999, **32**, 435.
5 M. Sofos, J. Goldberger, D. A. Stone, J. E. Allen, Q. Ma, D. J. Herman, W.-W. Tsai, L. J. Lauhon and S. I. Stupp, *Nat. Mater*., 2009, **8**, 68–75.
6 J. S. Kim, H. A. Marzouk, P. J. Reucroft and C. E. Jr Hamrin, *Thin Solid Films*, 1992, **217**, 133.
7 H. K. Ardakani, *Thin Solid Films*, 1996, **287**, 280.
8 A. Valentini, F. Quaranta, M. Penza and F. R. Rizzi, *J. Appl. Phys*., 1993, **73**, 1143.
9 Y. Lu, R. Ganguli, C. A. Drewien, M. T. Anderson, C. J. Brinker, W. Gong, Y. Guo, H. Soyez, B. Dunn, M. H. Huang and J. I. Zink, *Nature*, 1997, **389**, 364.
10 W. H. Li, E. W. Shi, W. Z. Zhong and Z. W. Yin, *J. Cryst. Growth*, 1999, **203**, 186.
11 (*a*) L. Vayssieres, K. Keis, S. E. Lindquist and A. Hagfeldt, *J. Phys. Chem. B*, 2001, **105**, 3350; (*b*) S. Yamabi and H. Imai, *J. Mater. Chem*., 2002, **12**, 3773; (*c*) L. Vayssieres, *Adv. Mater*., 2003, **15**, 464; (*d*) L. E. Greene, M. Law, J. Goldberger, F. Kim, J. C. Johnson, Y. Zhang, R. J. Saykally and P. Yang, *Angew. Chem., Int. Ed*., 2003, **42**, 3031; (*e*) Q. Li, V. Kumar, Y. Li, H. Zhang, T. J. Marks and R. P. H. Chang, *Chem. Mater*., 2005, **17**, 1001.
12 J. Yahiro, T. Kawano and H. Imai, *J. Colloid Interface Sci*., 2007, **310**, 302.
13 H. Usui, *J. Phys. Chem. C*, 2007, **111**, 9060.
14 A. Dev, S. K. Panda, S. Kar, S. Chakrabarti and S. Chaudhuri, *J. Phys. Chem. B*, 2006, **110**, 14266.
15 (*a*) P. Li, Y. Wei, H. Liu and X. Wang, *Chem. Commun*., 2004, 2856; (*b*) P. Li, Y. Wei, H. Liu and X. Wang, *J. Solid State Chem*., 2005, **178**, 855; (*c*) G. Sun, M. Cao, Y. Wang, C. Hu, Y. Liu, L. Ren and Z. Pu, *Mater. Lett*., 2006, **60**, 2777.
16 Z. R. Tian, J. A. Voigt, J. Liu, B. McKenzie and M. J. McDermott, *J. Am. Chem. Soc*., 2002, **124**, 12954–12955.
17 (*a*) M. Öner, J. Norwig, W. H. Meyer and G. Wegner, *Chem. Mater*., 1998, **10**, 460; (*b*) A. Taubert, G. Glasser and D. Palms, *Langmuir*, 2002, **18**, 4488.
18 (*a*) K. S. Choi, H. C. Lichtenegger, G. D. Stucky and E. W. McFarland, *J. Am. Chem. Soc*., 2002, **124**, 12402; (*b*) Y. Tan, E. M. P. Steinmiller and K.-S. Choi, *Langmuir*, 2005, **21**, 9618.
19 H. Usui, T. Sasaki and N. Koshizaki, *Appl. Phys. Lett*., 2005, **87**, 063105.
20 C. Liang, Y. Shimizu, M. Masuda, T. Sasaki and N. Koshizaki, *Chem. Mater*., 2004, **16**, 963.
21 R. P. Sperline, Y. Song and H. Freiser, *Langmuir*, 1997, **13**, 3727.
22 X. Gao, X. Li and W. Yu, *J. Phys. Chem. B*, 2005, **109**, 1155.
23 T. L. Sounart, J. Liu, J. A. Voigt, J. W. P. Hsu, E. D. Spoerke.
24 S. S. Rawat and A. J. Chattopadhway, *J. Fluoresc*., 1999, **9**, 233.
25 S. Hayashi and S. J. Ikeda, *J. Phys. Chem*., 1980, **84**(7), 744–751.
26 C. Boeckler, T. Oekermann, A. Fedhoff and M. Wark, *Langmuir*, 2006, **22**, 9427–9430.
27 J.-F. Liu and W. A. Ducker, *J. Phys. Chem. B*, 1999, **103**, 8558.

